Available online at www.sciencedirect.com

Catalysis Today 98 (2004) 413–421

www.elsevier.com/locate/cattod

Systematic evaluation of monometallic catalytic materials for lean-burn NO_x reduction using combinatorial methods

Kevin Krantz, Selim Senkan*

Department of Chemical Engineering, University of California, Box 951592, Los Angeles, CA 90095, USA

Abstract

A library of about 1000 distinct catalytic materials were prepared and tested systematically for their NO reduction activities using array channel microreactors and mass spectrometry. Catalysts were prepared by individually impregnating 42 elements from the periodic table into five support materials of γ-Al_2O_3, CeO_2, SiO_2, TiO_2 and Y-ZrO_2 at five different loadings. They were tested at 1 atm pressure, in the temperature range 100–500 °C, and at a GHSV of 60,000 h^{-1}. The feed gas used was 500 ppmv NO, 500 ppmv C_3H_6, 1400 ppmv CO, 8% O_2, 10% H_2O, and the balance helium. The most significant leads were Pt/TiO_2 and Pt/SiO_2, both of which exhibited superior performances, reducing the levels of NO by 25 and 20%, respectively.

1. Introduction

Recent developments in automotive engineering have made possible the production of more fuel efficient – up to 25% – lean-burning gasoline engines. However, the lack of appropriate catalytic technology to reduce NO_x emissions under lean-burn conditions impedes the commercialization of such engines [1]. In principle, NO_x reduction could be achieved by either decomposition of NO_x directly into N_2 and O_2 or by selective catalytic reduction (SCR) using hydrocarbons (HC), which are also present in the exhaust gases. The direct decomposition of NO_x is thermodynamically feasible below 900 °C ($\Delta G_f^\circ = -86$ kJ/mol), thus represents the best option for lean exhaust treatment [2]. However, because of the lack of progress in this approach, efforts were directed towards developing SCR-based technologies for NO_x reduction. These efforts were spurred by the discoveries that NO can selectively be reduced over Cu/ZSM-5 [3,4] and Pt–Al_2O_3 [5,6] by hydrocarbons such as C_2H_4, C_3H_6, C_3H_8. Alas, both of these materials subsequently were shown to possess considerable operational problems. For example, although Cu/ZSM-5 initially has high activity and selectivity, its activity severely decreases when exposed to steam, which is an inevitable combustion product. Platinum supported on Al_2O_3 is stable when exposed to steam, but its activity is restricted to a narrow temperature window, and also suffers from substantial N_2O production, which is a pollutant [6].

These early discoveries were then followed by decades long of impressive yet unsuccessful research with regard to the development of commercial lean-burn NO_x reduction catalysts. Although great strides have been made in understanding the fundamentals of NO reduction on an abundance of materials, such as the nature of adsorbed species, reaction mechanisms and solid structures (see for example the information chronicled in several excellent review papers [7–11]), this fundamental knowledge did not lend itself to the development of practical catalysts. We believe that one of the major reasons for this lack of progress has been the absence of a systematic and organized data base. For example, virtually all the results reported in the literature were derived from experiments conducted under different conditions in which different catalytic materials prepared by different methods were used. Consequently, the development of practical insights on structure activity relationships and reactivity trends has been extremely difficult.

The emergence of combinatorial or high throughput experimentation methods and tools now offer fresh new hopes to many pressing problems in catalytic science and technology [12], including NO_x reduction catalysis. In order

---

* Corresponding author. Tel.: +1 310 206 4106; fax: +1 310 267 0177. *E-mail address:* senkan@ucla.edu (S. Senkan).

0920-5861/$ – see front matter © 2004 Published by Elsevier B.V.
doi:10.1016/j.cattod.2004.08.009

to exploit this new methodology, we have developed array channel microreactors to rapidly screen libraries of catalytic materials [13], together with optical [14,15] and mass spectrometric [16] detection techniques. Previously we also reported on the feasibility of using array microreactors and MS as a rapid screening tool for NO_x reduction catalysis research [17].

In this communication, we now report the results of a systematic investigation of the catalytic activities of 42 elements from the periodic table individually impregnated on five porous oxide supports for the selective catalytic reduction of NO. All the catalytic materials were prepared and tested under identical and realistic conditions. Consequently, the results represent a useful data set to compare and assess the relative reactivity of elements on a variety of support materials as a function of metal loading and temperature. The present work reports results obtained using monometallic catalytic materials. Multimetallic combinations of catalytic materials will be the subject of future publications.

2. Experimental

2.1. Preparation of catalytic materials

Approximately 1000 distinct catalytic materials were prepared by individually impregnating 42 elements from the periodic table into five support materials at five different metal loadings. The powders of support materials (γ-Al_2O_3, CeO_2, SiO_2, TiO_2, Y-ZrO_2) were acquired from commercial vendors (see Table 1 for the properties of the supports). These materials were chosen because of their hydrothermal stability, availability and ability to be pelletized without a binder. The powders were then formed into 1 mm × 4 mm cylindrical pellets by a commercial press using a custom designed die and punch set. Forty six metal salt solutions were created for 42 elements from the periodic table as shown in Table 2. For K, In, Sn, and La multiple precursors were used. The metal salts were chosen so as to have adequate solubility, availability, and low toxicity. The salts had to be soluble enough to allow for high metal loadings on the pellets using microliter volumes of solution. Radioactive and toxic metals were disregarded from consideration for safety reasons. Predetermined quantities of stock solutions were introduced into the wells of a 96 chamber well-plate using a computer controlled liquid dispensation system (Cartesian Technologies, Inc., Irvine, CA). Five different concentrations of precursor solutions were used to prepare a library of catalytic materials, with metal loadings being in the range 0.001–25%, depending on the specific element and the support involved. This range of metal loading should create a good diversity of catalytic materials from well dispersed small metal/metal-oxide ensembles at low loading to large clusters at high loadings. After the stock solutions were dispensed, they were diluted, if necessary, to give 50 μL total solution on the well-plate. The pellets of support materials were then placed into the wells to affect impregnation. The pellets were soaked in the solutions for 72 h under an atmosphere of 100% relative humidity. Finally, the pellets were dried at 50 °C for 12 h, 80 °C for 12 h, 120 °C for 2 h, and calcined in air at 600 °C for 4 h. In some cases the supports were dissolved by the solutions used or were overloaded with the metal within a single impregnation step; these materials were discarded. Consequently for some metal–support combinations, less than five distinct materials were tested. In Table 2, the sources of metals and the specific metal loadings achieved on each support material are presented.

2.2. Screening of catalytic materials

The details of the catalyst screening system have been described before [17], thus only a brief description will be provided here. Catalytic materials were tested for their NO reduction activities using four ceramic microreactor arrays that were housed in a temperature controlled heating block, which was mounted on a precision *x*–*y*–*z*-motion control stage (Newmark Industries, Irvine, CA). Each array contained 20 microreactors, thus it was possible to screen up to 80 different catalysts in parallel. This capability, however, was not exploited as duplicates of catalytic materials and blank sites were employed during the screening process. Pellets of catalytic materials were placed into the cylindrical wells in each microreactor, over which the reactant gases passed, in a manner similar to monolithic catalytic reactors used in present day catalytic converters.

The reaction test conditions were chosen to be similar to an actual lean-burn automobile exhaust, with the following feed gas composition: 500 parts per million by volume (ppmv) NO, 500 ppmv C_3H_6, 1400 ppmv CO, 8% O_2, 10% H_2O, and the balance helium. In addition, the gas hourly space velocity (GHSV) was maintained at 60,000 h^{-1}, a value close to a commercial catalytic converter. Reactant gas flow rates were regulated using digital mass flow controllers

Table 1
Support materials and their properties

Material	Surface area (m^2/g)	Pellet weight (mg)	Source
γ-Al_2O_3, acidic, activated	128	23.4	Alfa-Aesar, Ward Hill, PA
CeO_2	17	61	Strem Chemicals, Newbury Port, MA
SiO_2, amorphous	400	9.6	Alfa-Aesar, Ward Hill, MA
TiO_2 (anatase)	268	11.7	Carbochem, Ardmore, PA
Y stabilized ZrO_2 (YSZ)	36	31.7	Stanford Materials Corp., Aliso Viejo, CA

Table 2
Sources of metals used and their loadings on support materials (wt.%)

Source/support loading (wt.%)	γ-Al_2O_3	CeO_2	SiO_2	TiO_2	Y-ZrO_2
$LiNO_3$	0.2, 1, 2, 5, 7.5	0.04, 0.5, 1, 2, 4.4	0.3, 1.5, 5, 10, 25	0.23, 2, 4.6, 10, 23	0.09, 0.9, 2, 4, 8.5
H_3BO_3	0.017, 0.07, 0.17, 0.5, 1.7	0.007, 0.026, 0.066, 0.2, 0.66	0.04, 0.2, 0.75, 2, 4.2	0.034, 0.14, 0.34, 1, 3.4	0.013, 0.05, 0.13, 0.38, 1.3
$NaNO_3$	0.5, 1, 2.6, 5, 9.7	0.2, 2, 4, 10, 20	1.2, 5, 10, 20, 50	1, 10, 20, 51, 102	0.4, 4, 8, 19, 38
$Mg(NO_3)_2$	0.1, 1, 2, 3.5, 7.5	0.04, 0.5, 1, 2, 3.7	0.24, 1.2, 5, 10, 24	0.2, 2, 4, 10, 20	0.07, 1.5, 3.5, 7
$Al(NO_3)_3$	n/a	0.01, 0.1, 0.2, 0.5, 1	0.07, 0.4, 1.5, 3, 6.8	0.06, 0.6, 1, 2.8, 5.6	0.02, 0.2, 0.4, 1, 2
KNO_3	0.25, 1, 1.6, 3, 6	0.05, 0.5, 1, 2, 5	0.3, 2, 5, 10, 25	0.25, 2.5, 5, 10, 25	0.09, 0.9, 2, 4.5, 9
$KOOC_2H_3$	0.5, 2.54.9, 9.8, 20	0.2, 2, 4, 10, 19	1.2, 5, 10, 20, 50	1, 10, 20, 49, 98	0.4, 4, 8, 18, 36
$Ca(NO_3)_2$	0.12, 1, 2, 4, 8	0.05, 0.5, 1, 2, 5	0.3, 2, 5, 10, 25	0.25, 2.5, 5, 12, 25	0.09, 0.9, 2, 4.5, 9
$Sc(NO_3)_2$	0.02, 0.2, 0.5, 1, 1.22	0.005, 0.01, 0.1, 0.2, 0.46	0.03, 0.15, 0.5, 1.5, 3	0.03, 0.3, 1, 2, 2.5	0.01, 0.05, 0.1, 0.5, 0.9
$(NH_4)_2TiO(C_2O_4)$	0.12, 0.25, 0.61, 1.2, 2.5	0.05, 0.5, 1, 2, 5	0.3, 2, 5, 10, 25	n/a	0.09, 0.9, 2, 4.5, 9
NH_4VO_3	0.004, 0.02, 0.05, 0.1, 0.2	0.004, 0.05, 0.1, 0.2, 0.4	0.01, 0.1, 0.5, 1,	0.008, 0.08, 0.16, 0.4, 0.82	0.007, 0.07, 0.15, 0.35, 0.7
$CrCl_2$	0.001, 0.01, 0.025, 0.05, 0.1	0.0004, 0.004, 0.008, 0.02, 0.04	0.003, 0.015, 0.05, 0.1, 0.27	0.002, 0.02, 0.04, 0.1, 0.2	0.0008, 0.009, 0.015, 0.04, 0.08
$MnCl_2$	0.5, 1, 2, 4.4, 8.8	0.2, 2, 4, 10, 19	1.2, 8, 15, 30, 50	1, 10, 20, 49, 98	0.36, 3.6, 8, 18, 36
$Fe(NO_3)_3$	0.4, 0.8, 1.6, 3, 5.1	0.15, 1.5, 3, 7, 15	1, 8, 15, 30, 50	0.8, 16, 39, 79	0.3, 3, 5.5, 14, 29
$Co(NO_3)_2$	0.64, 1.9, 3.8, 8.3, 15.4	0.25, 2.7, 5, 10, 24	1.6, 8, 15, 30, 50	1.3, 13, 26, 64, 128	0.5, 5, 10, 23, 47
$Ni(NO_3)_2$	0.5, 2, 3.9, 7.9, 15	0.2, 2, 4, 10, 19	1.2, 8, 15, 30, 50	1, 10, 20, 49, 98	0.36, 3.6, 8, 18, 36
$Cu(NO_3)_2$	0.64, 1.3, 2.6, 5.1, 10	0.24, 2.7, 5, 10, 24	1.6, 8, 15, 30, 50	1.3, 13, 26, 64, 128	0.5, 3.8, 8, 23, 47
Zn, plasma standard sol'n.	0.064, 0.51, 1, 2, 4.5	0.02, 0.27, 0.5, 1, 2.4	0.16, 1, 3.5, 7, 15.6	0.13, 1.3, 2.6, 6.4, 13	0.05, 0.4, 0.8, 2.3, 4.7
Ga, plasma standard sol'n.	0.02, 0.26, 0.5, 1, 2	0.008, 0.08, 0.16, 0.4, 0.8	0.05, 0.25, 1, 2.5, 5.2	0.043, 0.43, 0.86, 2.1, 4.3	0.016, 0.16, 0.3, 0.8, 1.6
Ge, plasma standard sol'n.	0.02, 0.2, 0.5, 1, 2.1	0.008, 0.08, 0.16, 0.4, 0.8	0.05, 0.25, 1, 2.5, 5.2	0.043, 0.43, 0.86, 2.2, 4.3	0.016, 0.16, 0.3, 0.8, 1.6
$RbNO_3$	1, 10, 20, 50, 98	0.4, 4, 7.5, 20, 37	2.4, 10, 20, 30, 50	2, 20, 40, 100, 197	0.7, 7, 14, 36, 72
$Sr(NO_3)_2$	0.64, 1.9, 3.8, 8.3, 15	0.25, 2.5, 5, 10, 24	1.6, 8, 15, 30, 50	1.3, 13, 26, 64, 128	0.5, 3.8, 8, 23, 47
$Y(NO_3)_3$	0.64, 1.9, 5.1, 10, 20	0.25, 2.5, 5, 10, 24	1.6, 8, 15, 30, 50	1.3, 13, 26, 64, 128	0.5, 3.8, 23, 47
$ZrCl_2O$	0.02, 0.1, 0.2, 0.5, 1	0.008, 0.08, 0.2, 0.4, 0.8	0.05, 0.5, 1, 2, 5.2	0.043, 0.43, 0.86, 2.1, 4.3	n/a
$NbCl_5$	0.02, 0.2, 0.5, 1, 2	0.008, 0.08, 0.2, 0.4, 0.8	0.05, 0.5, 1, 2, 5.2	0.043, 0.43, 0.86, 2.1, 4.3	0.016, 0.16, 0.3, 0.8, 1.6
$(NH_4)_6Mo_7O_{24}$	0.05, 0.5, 1, 2.5, 4.9	0.02, 0.2, 0.4, 1, 2	0.12, 1, 2, 5, 12	0.1, 1, 2, 4.9, 10	0.04, 0.4, 0.8, 1.8, 3.6
$(NH_4)_2RuCl_6$	0.0066, 0.072, 0.15, 0.3, 0.57	0.0025, 0.025, 0.05, 0.1, 0.25	0.016, 0.1, 0.25, 0.5, 1.6	0.01, 0.1, 0.3, 0.7, 1.3	0.005, 0.05, 0.1, 0.2, 0.5
$RhCl_3$	0.0082, 0.05, 0.15, 0.4, 0.8	0.003, 0.06, 0.15, 0.3	0.06, 0.25, 1, 2.5, 6	0.016, 0.16, 0.3, 0.8, 1.6	0.006, 0.06, 0.12, 0.3, 0.6
$PdCl_2$	0.043, 0.086, 0.21, 0.43, 0.85	0.02, 0.15, 0.3, 0.8, 1.6	0.1, 0.5, 1, 5, 10.4	0.085, 0.86, 1.7, 4.3, 8.5	0.03, 0.3, 0.6, 1.5, 3.2
$AgNO_3$	0.64, 1.3, 2.6, 5.1, 10	0.7, 2.7, 5, 10, 24	1.6, 6, 10, 15, 25	3.9, 13, 26, 64, 128	0.5, 3.8, 8, 23, 47
$InCl_3$	0.04, 0.26, 0.5, 1, 2	0.02, 0.15, 0.3, 0.8, 1.6	0.1, 0.5, 2, 5, 10.4	0.085, 0.86, 1.7, 4.3, 8.5	0.03, 0.3, 0.6, 1.5, 3.2
$In(NO_3)_3$	0.25, 1, 2.5, 7.4, 25	0.094, 0.4, 1, 3, 9.4	0.6, 2.4, 6, 10, 60	0.5, 2, 5, 10, 50	0.2, 0.7, 2, 5.4, 18
$SnCl_4$	0.45, 0.9, 1.3	0.17, 2, 4, 8, 17	1.1, 5, 10, 15, 25	0.9, 9, 18, 45, 89	0.3, 3, 6, 15, 33
$(NH_4)_2SnCl_6$	0.25, 0.5, 1	0.1, 1, 2, 4.5, 9	0.6, 2.5, 5, 10, 25	0.5, 5, 10, 25, 49	0.18, 1.8, 3.6, 9, 18
$Ba(NO_3)_2$	0.013, 0.1, 0.26, 0.5, 1	0.005, 0.05, 0.1, 0.25, 0.5	0.031, 0.15, 0.5, 1.5, 3.1	0.03, 0.3, 0.5, 1.3, 2.6	0.0095, 0.1, 0.2, 0.5, 1
$La(NO_3)_3$	0.5, 1.5, 3, 7, 14	0.2, 2, 4, 10, 20	1.25, 5, 10, 20, 30	1, 10, 21, 51, 103	0.4, 4, 8, 20, 38
$LaCl_3$	0.5, 1.5, 3.4, 6.9, 15	0.19, 2, 4, 10, 19	1.2, 5, 10, 20, 30	1, 10, 20, 49, 98	0.36, 3.6, 8, 18, 36
$Ce(NO_3)_3$	0.5, 2.5, 5, 10, 20	n/a	1.2, 5, 10, 20, 30	1, 10, 20, 49, 98	0.36, 3.6, 8, 18, 36
$Nd(NO_3)_3$	0.5, 2, 4, 8, 15	0.2, 2, 4, 8, 19	1.2, 5, 10, 20, 30	1, 10, 20, 49, 98	0.4, 2.9, 6.2, 18, 36
$Sm(NO_3)_3$	0.4, 3, 6, 13, 27	0.15, 1.5, 3, 7, 15	0.94, 4, 8, 16, 25	0.8, 8, 15, 38, 77	0.3, 2.6, 5, 15, 28
W, plasma standard sol'n.	0.002, 0.02, 0.05, 0.1, 0.2	0.0008, 0.01, 0.02, 0.04, 0.08	0.005, 0.025, 0.1, 0.25, 0.5	0.004, 0.04, 0.085, 0.21, 0.43	0.0016, 0.016, 0.03, 0.08, 0.16
$(NH_4)IrCl_6$	0.008, 0.05, 0.15, 0.4, 0.8	0.003, 0.03, 0.06, 0.15, 0.3	0.02, 0.1, 0.3, 1, 2	0.016, 0.16, 0.33, 0.8, 1.6	0.006, 0.06, 0.12, 0.3, 0.6
H_2PtCl_6	0.043, 0.13, 0.26, 0.5, 1	0.016, 0.15, 0.3, 0.8, 1.6	0.1, 0.5, 1, 3, 6	0.09, 0.9, 1.7, 4.3, 8.5	0.03, 0.3, 0.6, 1.5, 3
H_2AuCl_6	0.15, 0.25, 0.5, 1.2, 2.5	0.02, 0.2, 0.4, 1, 2	0.06, 0.25, 0.5, 2, 6.0	0.1, 1, 2, 4.9, 9.8	0.04, 0.4, 0.8, 1.8, 3.6
Pb, plasma standard sol'n.	0.02, 0.2, 0.5, 1, 2	0.008, 0.08, 0.16, 0.4, 0.8	0.052, 0.25, 0.5, 2, 5.2	0.04, 0.43, 0.9, 2, 4.3	0.016, 0.16, 0.3, 0.8, 1.6
$Bi(NO_3)_2$	0.02, 0.08, 0.2, 0.6, 2	0.0076, 0.03, 0.076, 0.23, 0.76	0.048, 0.2, 0.48, 1.4, 4.8	0.04, 0.16, 0.4, 1.2, 4.0	0.015, 0.06, 0.15, 0.44, 1.5

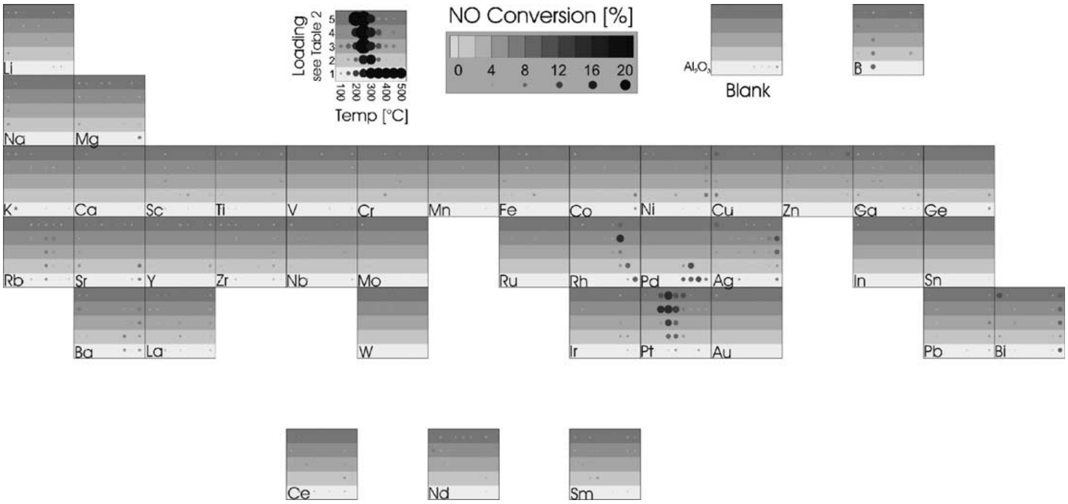

Fig. 1. Percent NO conversions for γ-Al_2O_3 supported catalytic materials. Larger and darker dots represent higher NO conversions.

(MKS, Inc., Andover, MA) and blended using a static mixer. Steam was generated within the preheater section of the reactor block and mixed with the reactants prior to entering the back of the reactor arrays. Experiments were performed under 1 atm pressure from 100 to 500 °C with 50 °C increments and back down to 200 °C in 100 °C increments over 24 h period in order to also assess catalyst stability. This time frame was previously shown to be adequate to determine the deactivation rates of some catalytic materials, e.g.Cu/ZSM-5, under similar reaction conditions [17].

Product gases exiting the microreactor channels were sequentially withdrawn by a heated capillary sampling line and analyzed immediately by a mass spectrometer (Stanford Research Systems, RGA-200, Sunnyvale, CA). The mass spectrum covering the 2–50 amu range was scanned four times for each reactor channel and averaged to improve signal to noise ratio. It was possible to screen the entire 80 site library at one temperature in about 1 h. Nitric oxide and propylene concentrations were determined by monitoring masses 30 and 41 amu, respectively. We were not able to unambiguously monitor the CO levels in the current experimental system because of signal contaminations from C_3H_6 fragmentation and atmospheric N_2 diffusion. Although the formation of other species, such as NO_2 and N_2O, may also contribute to the mass 30 signal, monitoring mass 30 has been shown to represent a good primary screening diagnostic to assess NO elimination. The concentration of N_2O was not determined because its mass spectrum overlaps not only with NO but also with CO_2. The individual reactor signals were referenced to an empty site in each reactor array to remove the influence of possible homogeneous reactions, blank reactor activity, and experiment-to-experiment variations.

3. Results and discussion

In Fig. 1 the percent reduction in NO concentrations for each of the 42 elements supported on γ-Al_2O_3 are presented

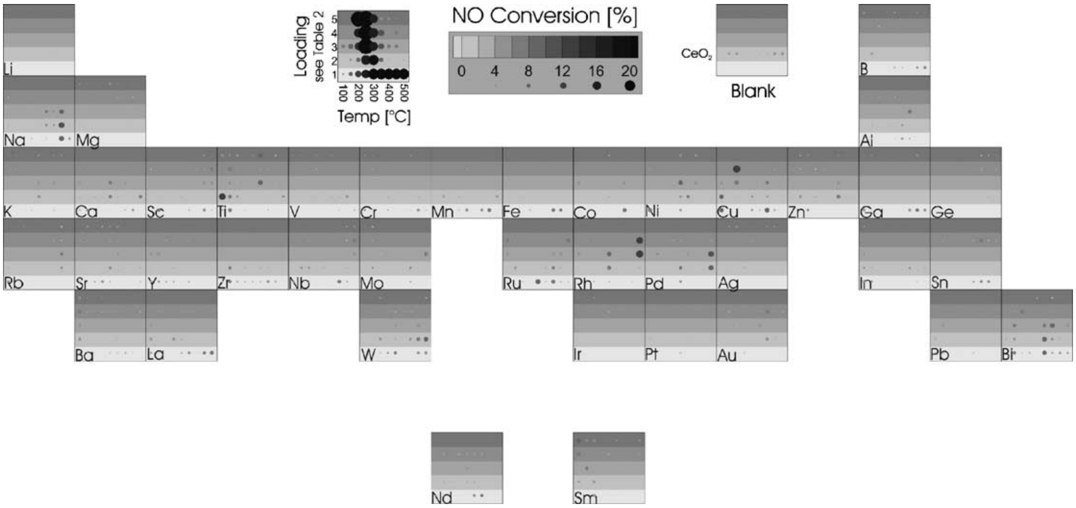

Fig. 2. Percent NO conversion for CeO_2 supported catalytic materials. Larger and darker dots represent higher NO conversions.

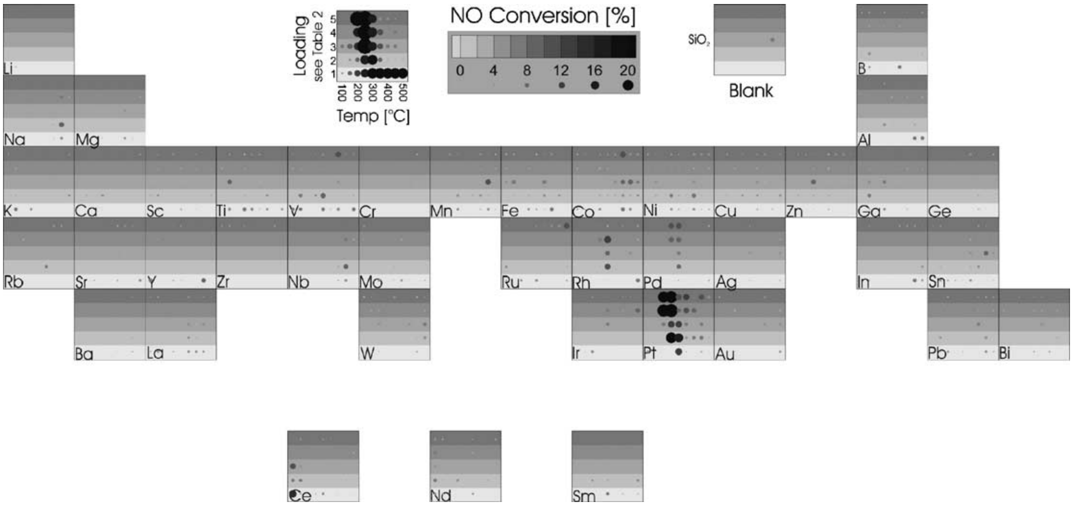

Fig. 3. Percent NO conversion for SiO_2 supported catalysts. Larger, darker dots represent higher NO conversions.

in the periodic table format. In this and subsequent figures, higher NO reduction levels are indicated by larger and darker dots, in accordance with the legend insert shown. As indicated in the legend, the maximum percent NO reduction was about 20% under the experimental conditions investigated. Within each elemental square data set, rows of data in the increasing *y*-direction represent higher metal loadings in accordance with the values presented in Table 2. Similarly, the columns of data from left to right correspond to different temperatures from 100 to 500 °C in 50 °C intervals. The NO reduction data for the remaining support materials are presented in Figs. 2–5, respectively.

In Figs. 6–10, percent C_3H_6 conversions are similarly presented for the 42 elements in the periodic table format for each of the five supports. Although the data are presented in a format identical to NO reduction, the conversion maxima for C_3H_6 were 100%. That is, the largest and darkest dots in Figs. 6–10 represent 100%, as opposed to 20% that were the case in Figs. 1–5. In the following discussion, some of the highlights of this systematic data set are presented.

An inspection of Figs. 1–5 readily reveals that platinum group of metals, in general, exhibit the best NO reduction activities on SiO_2 and TiO_2, and to a lesser extent on γ-Al_2O_3. In particular, Pt/SiO_2 (Fig. 3) and Pt/TiO_2 (Fig. 4) stands out, providing NO reduction levels in excess of 20 and 25%, respectively. In comparison, the Pt/γ-Al_2O_3 (Fig. 1), a widely studied standard material, did not perform as well, reducing NO by only 10–15% under the identical conditions investigated. As seen in Figs. 3 and 4, the effectiveness of Pt/TiO_2 and Pt/SiO_2 were highest at higher Pt loadings. Both types of catalytic materials also exhibited excellent NO reduction activities over a broad temperature range of 100–400 °C, with the peak activity around 250 °C, shifting to slightly lower temperatures with increased Pt loading. These results are consistent with the results of Pt-

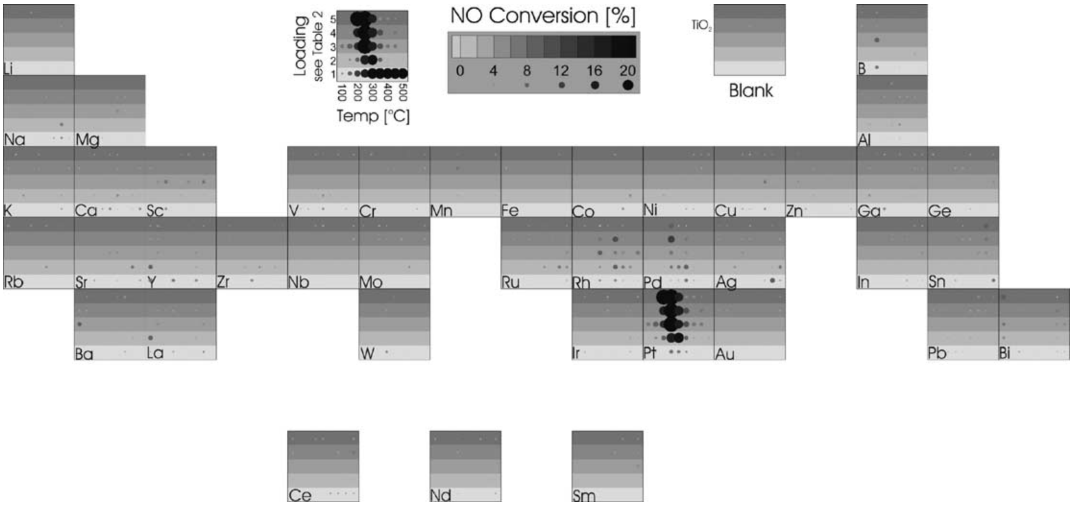

Fig. 4. Percent NO conversion for TiO_2 supported catalysts. Larger, darker dots represent higher NO conversions.

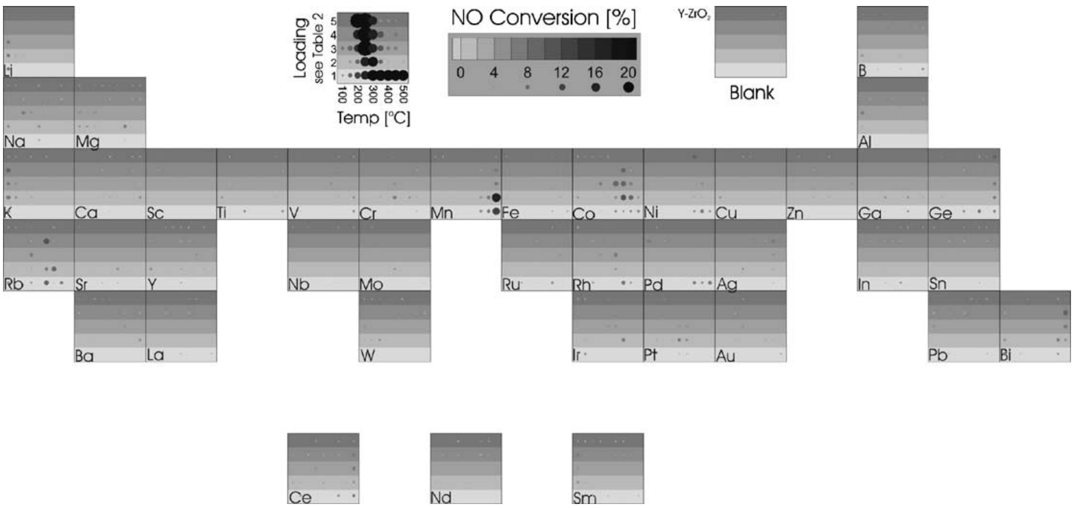

Fig. 5. Percent NO conversion for Y-ZrO$_2$ supported catalysts. Larger, darker dots represent higher NO conversions.

based catalytic materials reported in the literature [18]. It is particularly interesting to note that compared to TiO$_2$ and SiO$_2$, the Pt/γ-Al$_2$O$_3$ exhibited a narrower temperature window of 200–350 °C, an expected result based on prior studies [5,6]. These results clearly indicate the superiority of titania and silica as support materials for Pt in the SCR of NO. As seen in Figs. 6, 8 and 9 all of the Pt/γ-Al$_2$O$_3$, Pt/TiO$_2$ and Pt/SiO$_2$ catalysts also resulted in substantial propylene conversion (combustion), with light-off temperatures shifting to lower values with increasing Pt loading. For example, for the case of the Pt/γ-Al$_2$O$_3$, the light-off temperature decreased from 350 °C at 0.043% Pt loading to 200 °C at 1% Pt loading. Neither TiO$_2$ nor SiO$_2$ supported Pt catalysts exhibited measurable deactivation over the duration of the screening experiments, i.e. 24 h period. As noted earlier, Pt supported catalysts can transform NO to N$_2$O. Although not measured, this is most likely occurring in the present set of Pt-based catalysts as well. A more complete analysis of the reaction products clearly needs to be performed in subsequent studies, to better evaluate the most promising leads reported here.

In contrast, Pt/Y-ZrO$_2$ gave trace NO conversion (Fig. 5), but propylene conversions were complete at higher temperatures for all but the lowest loadings of Pt (Fig. 10). On the other hand, Pt–CeO$_2$ catalysts were not effective at all in reducing NO (Fig. 2), and also failed to provide complete propylene conversion within the temperature range considered (Fig. 7). The latter results are also consistent with the fact that ceria can inhibit the oxidation ability of platinum [19].

Palladium also gave some measurable NO reduction activity on all support materials except zirconia. The maximum NO conversion for each support was approximately 10%. However, the temperature for the maximum NO conversion and the temperature windows were significantly different for each support. On alumina, the

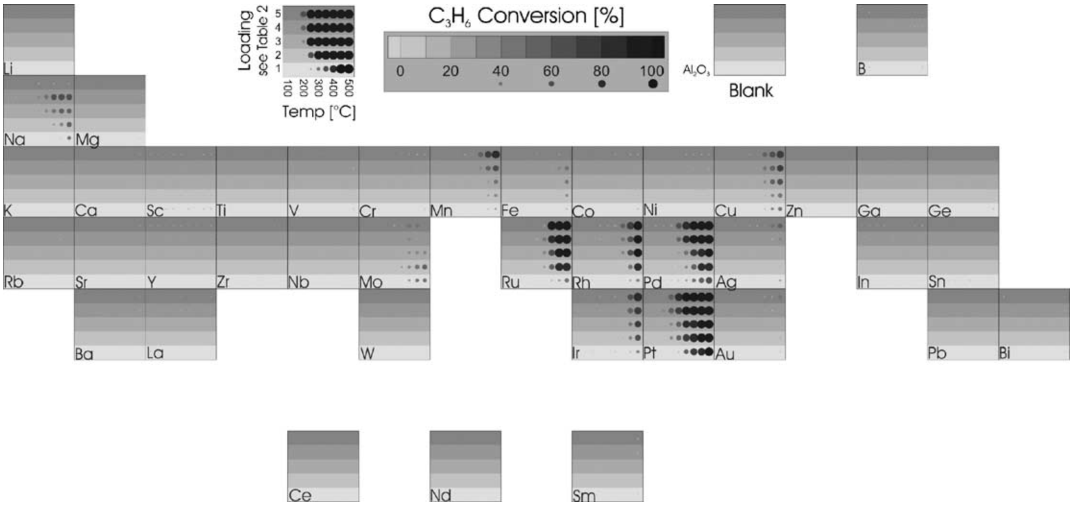

Fig. 6. Percent C$_3$H$_6$ conversion for γ-Al$_2$O$_3$ supported catalysts. Larger, darker dots represent higher C$_3$H$_6$ conversions.

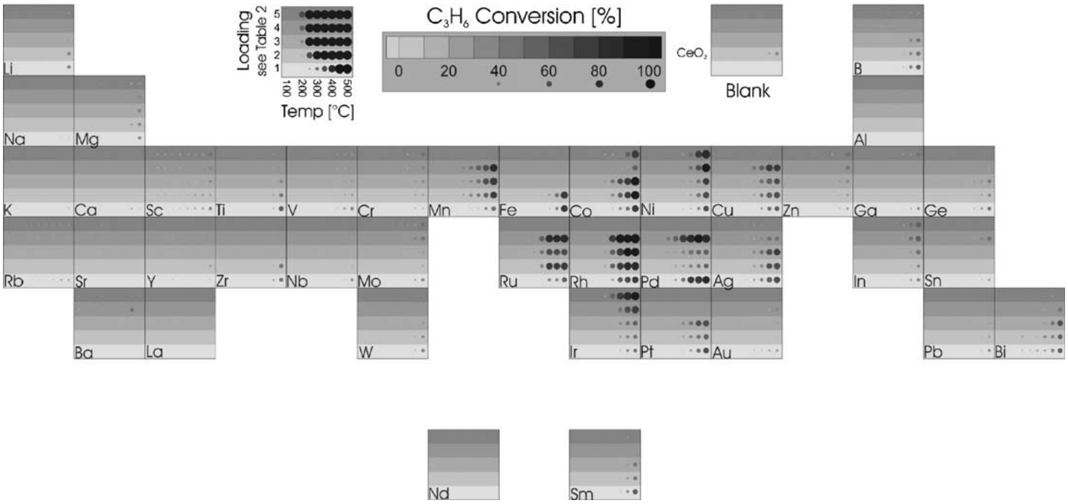

Fig. 7. Percent C_3H_6 conversion for CeO_2 supported catalysts. Larger, darker dots represent higher C_3H_6 conversions.

maximum NO conversion occurred at 400–450 °C, while on silica and titania, the maximum conversions occurred at lower temperatures in the 250–300 °C range. For alumina, the best performers were the lowest Pd loadings of 0.043 and 0.086%, while for silica the highest Pd loadings of 5 and 10.4% resulted in the highest NO reduction. These results clearly illustrate the importance of metal–support interactions. On titania, the Pd loading level differences caused a 100 °C shift in the temperature maxima for NO conversion and a narrowing of the temperature window as the loading increased from 0.086 to 0.86 and to 8.6% Pd/TiO_2. These results are also consistent with the propylene conversion profiles. For example, the materials with lowest Pd/TiO_2 loadings never achieved 100% C_3H_6 conversion even at 500 °C. The $Y\text{-}ZrO_2$ supported Pd catalysts did not substantially convert NO (Fig. 5), but they did have high hydrocarbon conversion activities (Fig. 10).

Rhodium was also an effective SCR catalyst for NO on several different supports. For example, 0.4% $Rh/\gamma\text{-}Al_2O_3$ (Fig. 1) led to a 15% reduction in NO levels at 400 °C. Similarly, 0.8% Rh/TiO_2 (Fig. 4) reduced the levels of NO by 10% at 350 °C. As seen in Fig. 9, only the highest Rh loaded titania (1.6% Rh/TiO_2) achieved the complete hydrocarbon conversion within the temperature range investigated. For the silica support, the Rh loadings of 0.25, 1, and 2.5% produced a maximum NO conversion of about 10% at 300 °C (Fig. 3). Because of its excellent NO reduction capabilities in stoichiometric combustion

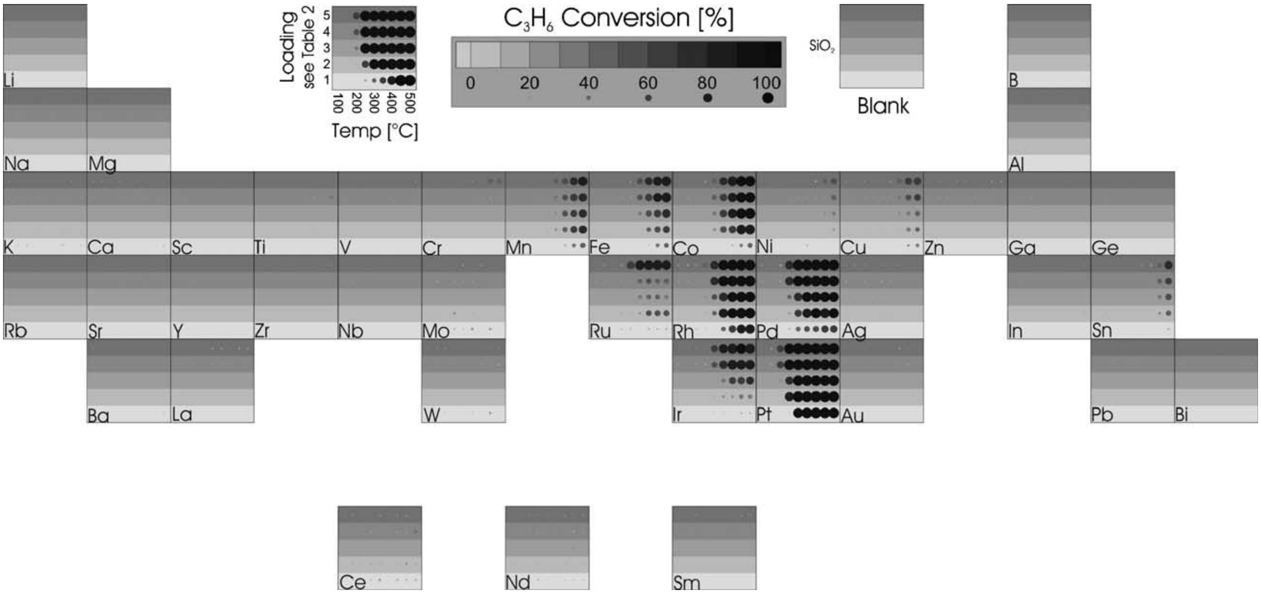

Fig. 8. Percent C_3H_6 conversion for SiO_2 supported catalysts. Larger, darker dots represent higher C_3H_6 conversions.

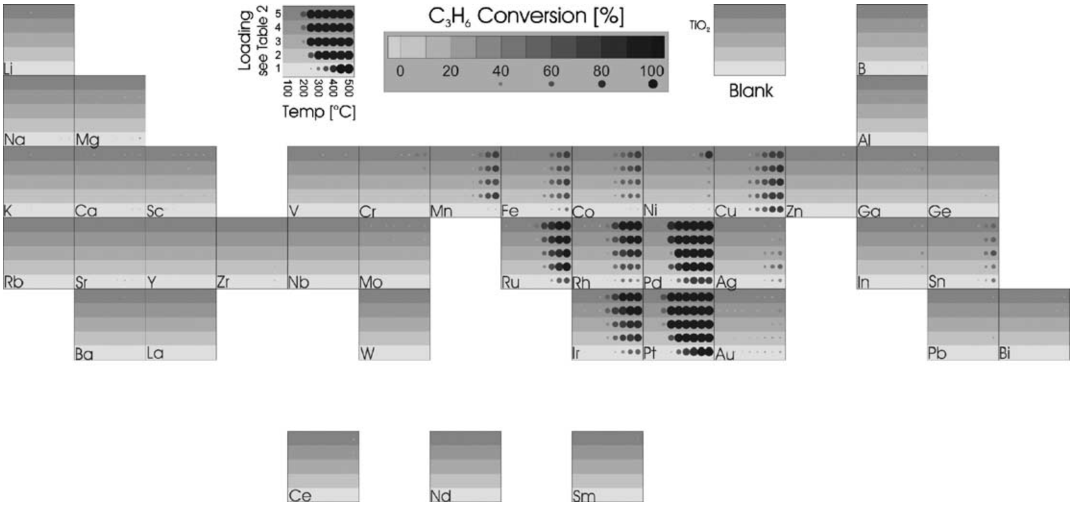

Fig. 9. Percent C_3H_6 conversion for TiO_2 supported catalysts. Larger, darker dots represent higher C_3H_6 conversions.

exhausts, Rh remain an important component in present day three-way catalysts [20].

Additional catalytic materials that exhibited notable NO reduction activities were Na/CeO_2 (10% at 450 °C) and Cu/CeO_2 (10% at 200 °C) (Fig. 2), and Rb/Y-ZrO_2 (10% at 350 °C) and Mn/Y-ZrO_2 (15% at 500 °C) and Co/Y-ZrO_2 (10% at 350 °C) (Fig. 5). The ceria supported alkali metals exhibited NO reduction only at the higher temperatures explored (i.e. 450–500 °C). Manganese is known to be a good catalyst for the oxidation of NO to NO_2 and according to one of the proposed mechanisms for NO reduction, the first step would be to oxidize NO to NO_2 [21]. In fact, other researchers have created bifunctional catalyst mixtures where manganese oxide is combined with another catalytic component to enhance the overall reduction of nitric oxide [21–23]. We also confirmed the formation of NO_2 in our Mn-containing catalysts by noting the increased intensity for the mass number 46 signal, the parent peak for NO_2. A thermodynamic analysis of the NO oxidation reaction show that even at 500 °C, the formation of NO_2 cannot be ruled out. This clearly calls for the undertaking of additional experiments to better establish the product distributions, for example by gas chromatography. It is interesting to note from Figs. 6–10 that although Mn is an active metal for propylene conversions on all supports, little or no NO conversion occurs on supports other than Y-ZrO_2.

Cobalt was also noted to be an active NO reduction catalyst when supported on Y-ZrO_2 (Fig. 5) or SiO_2 (Fig. 3). The maximum NO conversion for either of these support were about 10% within the 350–450 °C range. It has been suggested that the key to creating cobalt catalysts with high activity involves keeping the cobalt particles well dispersed and isolated to prevent the formation of Co_3O_4 because Co^{2+} is the active form of cobalt [24]. Since Co loadings were

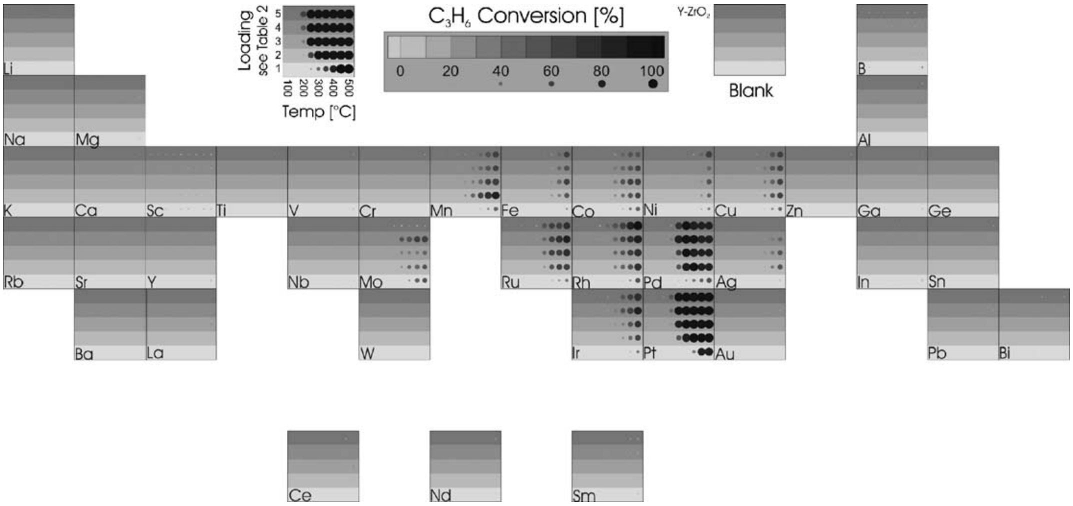

Fig. 10. Percent C_3H_6 conversion for Y-ZrO_2 supported catalysts. Larger, darker dots represent higher C_3H_6 conversions.

high in our experiments, we would not expect to see such a trend in our results. In fact, catalytic materials which provided the largest NO conversion had the highest Co loading for the silica support, and there was no discernible trend with respect to loading for the zirconia based catalysts (Fig. 5).

Catalytic materials containing Co are also known to produce NO_2 from NO [25]. Again, this was confirmed in our experiments by the detection of significant levels of mass number 46 among the reaction products from Co/Y-ZrO_2, Co/SiO_2 and Co/γ-Al_2O_3. Propylene conversions were insignificant over Co/γ-Al_2O_3 (Fig. 6) and never reached 100% over Co/Y-ZrO_2 even at the highest temperatures investigated (Fig. 10). However, complete propylene conversions were achievable over Co/SiO_2 at high Co loadings and at higher temperatures (Fig. 8).

In summary, a comprehensive and systematic investigation of the catalytic activities of 42 elements from the periodic table impregnated into five different porous support materials revealed several new leads for the SCR of NO in the presence of a large abundance of O_2. Among the most significant findings were Pt/TiO_2 and Pt/SiO_2, both of which exhibited superior NO reduction performances when compared to the traditional Pt/γ-Al_2O_3. These initial leads clearly must be followed up by more detailed analytical studies to better quantify the reaction products and to characterize the structures of the catalytic materials. For example, it would be useful to determine the levels of N_2O, CO and CO_2 in the experiments together with those for C_3H_6 presented here, as well as the precise breakdown of reaction products. In addition, the characterization of the lead catalytic materials with regard to the distribution of metals across the support and their cluster sizes would be useful to prepare improved catalytic materials. Finally, the undertaking of more extensive durability tests will be needed to determine the practical viability of the catalytic materials.

Acknowledgments

This research was supported, in part, by the National Science Foundation and the US Environmental Protection Agency. The authors also thank Drs. Isik Onal and Sukru Ozturk for useful discussions.

References

[1] R.J. Farrauto, R.M. Heck, Catal. Today 51 (1999) 351.

[2] S. Bhattacharyya, R.K. Das, Int. J. Energy Res. 23 (1999) 351.

[3] W. Held, A. Koenig, T. Richter, L. Puppe, SAE Paper, 900496, 1990.

[4] S. Sato, Y. Yu-u, H. Yahiro, N. Mizuno, M. Iwamoto, Appl. Catal. 70 (1991) 1.

[5] H. Hamada, Y. Kintaichi, M. Sasaki, T. Ito, Appl. Catal. 75 (1991) 1.

[6] A. Obuchi, A. Ohi, M. Nakamura, A. Ogata, K. Mizuno, H. Ohuchi, Appl. Catal. B 2 (1993) 71.

[7] M. Shelef, Chem. Rev. 95 (1995) 209.

[8] A. Fritz, V. Pitchon, Appl. Catal. B 13 (1997) 1.

[9] V.I. Parvulescu, P. Grange, B. Delmon, Catal. Today 46 (1998) 233.

[10] H. Akama, K. Matsushita, Catal. Surv. Jpn. 3 (1999) 139.

[11] M.D. Amiridis, T. Zhang, R.J. Farrauto, Appl. Catal. B 10 (1996) 203.

[12] S. Senkan, Angew. Chem. Int. Ed. Engl. 40 (2001) 312.

[13] S. Senkan, S. Ozturk, Angew. Chem. Int. Ed. Engl. 38 (1999) 791.

[14] S. Senkan, Nature 394 (1998) 350.

[15] S. Senkan, S. Ozturk, K. Krantz, I. Onal, Appl. Catal. A 254 (2003) 97.

[16] S. Senkan, K. Krantz, S. Ozturk, V. Zengin, I. Onal, Angew. Chem. Int. Ed. Engl. 38 (1999) 2794.

[17] K. Krantz, S. Ozturk, S. Senkan, Catal. Today 62 (2000) 281;
S. Ozturk, S. Senkan, Appl. Catal. B: Environ. 38 (2002) 243.

[18] R. Burch, P.J. Millington, Catal. Today 29 (1996) 37.

[19] Y.F. Yu-Yao, Ind. Eng. Chem. Prod. Res. Dev. 19 (1980) 293.

[20] M. Shelef, G.W. Graham, Catal. Rev.-Sci. Eng. (1994) 433.

[21] M. Misono, Y. Hirao, C. Yokoyama, Catal. Today 38 (1997) 157.

[22] T.-W. Kim, M.-W. Song, H.-L. Koh, K.-L. Kim, Appl. Catal. A 210 (2001) 35.

[23] I.-S. Nam, M.H. Kim, Korean J. Chem. Eng. 18 (2001) 725.

[24] J. Yan, M.C. Kung, W.M.H. Sachtler, H.H. Kung, J. Catal. 172 (1997) 178.

[25] F.C. Meunier, V. Zuzaniuk, J.P. Breen, M. Olsson, J.R.H. Ross, Catal. Today 59 (2000) 87.